Effect of Constitutive Behaviour of Strata on the Prediction of Subsidence Above Single-seam and Multi-seam Supercritical Longwall Panels

A M Suchowerska, CGMM[1], University of Newcastle
J P Carter, CGMM, University of Newcastle
J P Hambleton, CGMM, University of Newcastle
RS Merifield, SMEC Australia Pty Ltd

Summary

Numerical methods have the potential to assist in prediction of subsidence, particularly in new mining environments such as multi-seam mining. However, numerical methods have often been criticised for the predictions of subsidence above single-seam longwalls not matching field measurements well. To achieve a realistic prediction, a sound understanding of the mechanical laws governing the deformation of the sub-surface strata is required. Within the framework of the finite element method (FEM), this study compares predicted subsidence profiles, as well as stress distributions in the sub-surface strata, for a selection of the different constitutive laws currently used by practising engineers to represent coal measure strata. Further, a strain-stiffening caved goaf material is introduced into the simulations to allow the vertical stresses along the longwall floor to return to the original overburden load. Both single seam and multi-seam longwall panels are considered. A key finding is that the best agreement between predictions and field observations of subsidence is when the coal measure strata are represented as an elastic material with closely spaced frictionless horizontal interfaces, representing bedding planes. With this model the vertical stress also returns to the overburden stress in the caved goaf material within the first seam, prior to extraction of the second seam. The results show that more sophisticated and numerically taxing constitutive laws do not necessarily lead to more accurate predictions of subsidence when compared to field measurements. The advantages and limitations of using each particular constitutive law considered in the study are presented.

1. Introduction

Empirical and numerical models are typically used to predict subsidence due to longwall coal mining, yet they differ widely in terms of how they consider the influencing factors (e.g., overburden depth, longwall panel width, strength and deformability of strata, stratigraphy, etc.). Empirical methods are usually based on direct relationships determined through limited observations or measurements, which restrict the development of our understanding of how all the influencing factors interact to govern the mechanics of the system. The site-specific nature of empirical data also makes it difficult to transfer available empirical relationships to new mining environments. In the case of multi-seam longwall mining, the limited number of multi-seam mining cases in Australia means that proven empirical methods are not yet available to use for this new mining environment (Li et al., 2007).

In general, there has been poor agreement of predictions of subsidence using numerical methods with measurements made in the field, irrespective of which numerical modelling method was used (Coulthard et al., 1988; Kay et al., 1991; Mohammad et al., 1998; Esterhuizen et al., 2010). Currently, the primary limitation in obtaining accurate predictions of subsidence using numerical modelling methods has been identified as the

[1] Priority Research Centre for Geotechnical and Materials Modelling

lack of constitutive laws that realistically represent coal measure strata. More sophisticated constitutive laws are becoming increasingly popular amongst numerical modellers, even though they are numerically expensive and generally take a long period of time to run. Although there have been numerous subsidence studies conducted for a range of constitutive laws (e.g. Kay et al 1991; Lloyd et al 1997; Coulthard et al 2008), there has been no single study conducted nor aggregation of results from previous studies that provides a comprehensive assessment of the effect of numerically expensive constitutive laws on the accuracy of predicted subsidence and subsurface displacements.

This paper assesses the effects of differing assumptions for the constitutive laws, used to represent the coal measure strata and caved goaf, on the accuracy of the predicted subsidence above longwall mining when compared with field measurements. Supercritical longwall panel extraction is considered for single-seam and multi-seam arrangements, as schematically shown in Figure 1(a) and (b), respectively.

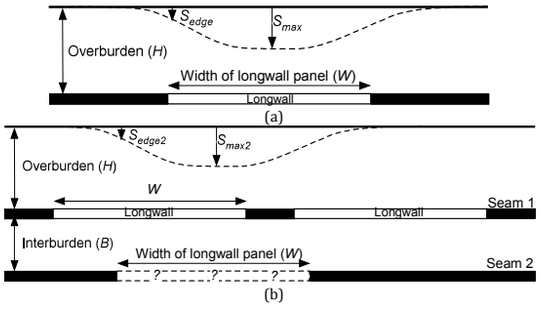

Figure 1 **Schematic diagram of problems analysed in this paper for (a) single-seam mining and (b) multi-seam mining**

Plane strain conditions are assumed. The overburden above the longwall panel is considered as three mechanically different materials: a purely isotropic linear-elastic material, an elastoplastic material and a jointed material. Some models include a strain-stiffening material to represent the goaf material that collapses onto the floor of the first-mined seam. The trends typically observed in field measurements of subsidence above single-seam mining are used to infer the possible material behaviour of coal measure strata. The constitutive laws used to represent the deformation of the subsurface strata are assessed to determine if they can accurately predict the vertical stress distribution on the longwall floor of the first seam, as this is deemed important for accurate prediction of subsidence above multi-seam longwall panels.

2. Background

2.1 Subsidence above single-seam longwall panels

Empirical data has shown that the key factors that govern the shape and magnitude of subsidence above single-seam longwall panels include the geometry of the extracted area of coal, the overburden geology and the surface topography (McNally et al 1996; Mills et al 2009). The so-called critical width is the ratio of width of a longwall panel *(W)* to overburden depth *(H)* at which maximum possible subsidence is reached (Mills et al 2009). In many of the coalfields in Australia, critical widths of longwall panels correspond to a ratio $(W/H)_{crit}$ of 1.0 to 1.6 (McNally et al 1996; Mine Subsidence Engineering Consultants 2007; Mills et al 2009). In the Southern and Western Coalfields of NSW, the maximum subsidence above a supercritical longwall panel in the first seam (S_{max1}) is approximately 55-65% of the first seam's extracted thickness (T_1) (Mine Subsidence Engineering Consultants 2007; Mills et al 2009). The maximum subsidence above the edge of the longwall panel (S_{edge}) has been recorded to be within the range of 5 to 15% of S_{max} (Holla 1985; Holla 1987; Coulthard et al 1988; Holla 1991). It is important to remember that these trends should only be considered as being general, as surface topography and unusual geological features can lead to anomalies in subsidence profiles (Kay et al 1992; McNally et al 1996; Holla et al 2000).

2.2 Subsidence above multi-seam longwall panels

The subsidence profiles recorded above multi-seam longwalls indicate that they differ with respect to both shape and magnitude compared to those observed above single-seam longwall panels. Recorded measurements of maximum incremental subsidence above multi-seam supercritical longwall (S_{max2}) are typically larger than those recorded above single-seam mining, in the order of 80% of the extracted seam height of the

second seam (T_2) (Schumann 1987; Dynl 1991; Sheorey et al 2000; Li et al 2007; Mine Subsidence Engineering Consultants 2007; te Kook et al 2008). An exception is multi-seam mining in the coalfields of the United Kingdom, where typical magnitudes of maximum subsidence above the second seam longwall extraction are similar to those recorded above longwalls in the first seam. These findings of increased subsidence upon extraction of longwalls in the second seam have typically been from coalfields where the geology of the overburden strata is relatively competent and subsidence in the first seam is usually in the order of 50-65% of the extracted seam thickness of the first seam (T_1). The subsidence profiles recorded above multi-seam longwall panels have been hypothesized to be influenced by the thickness and geology of the interburden and the relative orientation of the longwalls in each seam (Li, Steuart et al 2007; Mine Subsidence Engineering Consultants 2007), in addition to the parameters that influence subsidence above single-seam mining.

The simplest arrangement of longwalls in multiple seams is where the longwalls are parallel and the longwalls lie directly over each other. This arrangement is also referred to as a stacked arrangement and has been used in Sigma Colliery in South Africa (Schumann 1987; Li et al2007) and Newstan Colliery in NSW (Mine Subsidence Engineering Consultants 2012).

In the former location the longwall panels were the same width in each seam and the maximum incremental subsidence upon extraction of the second seam longwall (S_{max2}) occurred above the centre of the second-seam longwall panel. In the latter location, the width of the longwall located in the second seam was 1.4 times the width of the longwall located in the first seam. The maximum incremental subsidence above the second extracted seam (S_{max2}) occurred above the edges of the first seam longwall panel, where low values of subsidence were observed after extraction of the first seam. It was also noted that the magnitude of the incremental subsidence recorded above the second seam panel underlying the first seam longwall panel was larger than when underlying a chain pillar. These results suggest that some component of additional vertical movement is occurring in the goaf material of the first seam longwall panel while mining the second seam. Other field measurements have supported this idea that the first seam goaf remobilises and undergoes additional compaction (Bai et al 1995; Gale 2004; Li et al 2007; Mine Subsidence Engineering Consultants 2007).

For the few accounts of subsidence profiles recorded above multi-seam longwall panels in NSW, Australia, the shape and magnitudes cannot be predicted using the methods currently used for single-seam mining (Li et al 2007; Mine Subsidence Engineering Consultants 2007). The lack of a comprehensive database is the current limitation for the use of empirically derived relationships. Therefore, there is a need to investigate what numerical methods can accurately predict the subsidence above multi-seam longwall panels.

2.3 Prediction of subsidence using finite element method

Numerical methods aim to find the accurate prediction of subsidence by modelling the stress distribution and associated displacements as a result of extracting coal from a longwall panel. A realistic representation of the longwall mining process would require a three-dimensional model with progressive coal extraction and accurate location and properties of discontinuities present in the coal measure strata. However, three-dimensional models can be prohibitively difficult to construct, and three-dimensional analyses require substantially longer run times compared to two-dimensional models. Further, the accuracy of the solution from such an explicit three-dimensional model is highly dependent on realistic constitutive laws being used to represent the mechanics of the coal measure strata. Subsidence profiles can be predicted assuming plane strain (two-dimensional) conditions for the numerical model. Models have been considered of both the transverse cross section (i.e. parallel to the advancing face) or of the longitudinal cross-section (i.e. a slice through the centre of the longwall). To capture the subsidence profile with the largest change in tilt, the transverse cross-section is considered in this study.

It has long been known that when the coal measure strata are represented by the simplest mechanical behaviour, such as an isotropic linear-

elastic material, the predicted subsidence profile is shallower and wider than observed in the field. When a suitably small enough Young's modulus *(E)* is selected to yield an appropriate magnitude of maximum subsidence, the predicted subsidence profile overestimates the subsidence at the panel edges (Coulthard et al 1988; Kay et al 1991). The effect of representing the overburden as an isotropic elastic, transversely isotropic or elastic-perfectly plastic materials on the accuracy of subsidence predictions was studied more than a decade ago (Fitzpatrick et al 1986; Coulthard et al 1988; Kay et al 1991; Su 1991). The transversely isotropic material gave the best agreement when compared with field measurements. However, all of these studies considered a model where the extracted seam was left as a void and allowed for the overburden to sag the full extraction height. Most of the models would not have predicted a return to overburden stress along the longwall floor because the overburden would not have sagged enough for the longwall roof to come in contact with the longwall floor.

Results have suggested that better agreement between numerical modelling predictions and field measurements can be achieved when representing the coal measure strata using more sophisticated constitutive laws (Coulthard et al 1988; Mohammad et al 1998; Gale 2011). These more sophisticated constitutive laws have consisted of a combination of numerically expensive relationships, e.g. elastoplastic, strain-softening, ubiquitous joint elements, coupled rock failure and fluid flow systems (Lloyd et al 1997; Gale 2004; Esterhuizen et al 2010; Vakili et al.2010).

The limitation of most reports and papers describing numerical models that used numerically expensive constitutive laws is that it is often unclear what the relative contributions of each of the components of the material response and their properties are to the overall mechanics of the subsurface strata deformations and magnitude of the predicted subsidence profile. Some of these numerically expensive constitutive laws will be defined further below.

2.4 Constitutive laws for coal measure strata

2.4.1 Elastic-perfectly plastic model

An elastoplastic material is one which will behave elastically until it reaches yield, after which it will behave plastically. Yield is defined by a failure criterion, which for rock is often the Mohr-Coulomb failure criterion. For an elastic-perfectly plastic material, the yield criterion or yield surface does not change with plastic straining. At yield, a perfectly plastic material is assumed to flow at constant stress with no deformation limit. A schematic representation of the relationship of stress to strain for an elastic-perfectly plastic material is given in Figure 2(a).

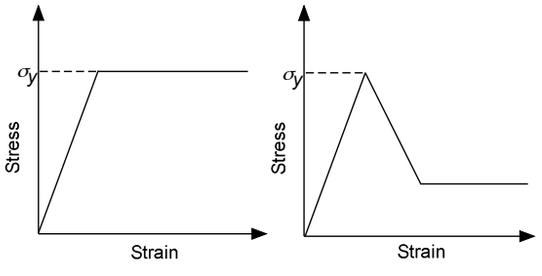

Figure 2 **Schematic diagram of stress-strain relationship for: (a) elastic-perfectly plastic and (b) elastoplastic strain-softening**

2.4.2 Elastoplastic strain-softening model

For an elastoplastic strain-softening material, the yield surface contracts with plastic straining (Yu 2010). In the elastic phase the material behaves in the same manner as an elastic-perfectly plastic material. It differs in the plastic phase, where plastic straining reduces the strength of the material (Figure 2(b)). The term softening is often used as the yielded material is no longer able to support the stress that initially caused it to yield and so the stress needs to be redistributed elsewhere. The reduction of strength can be applied to any of the strength parameters (e.g. φ, c) and be expressed as a function of the plastic strain (ε_p). Strain-softening has been used in numerical models for rock mechanics problems to represent the brittle nature of the failure of rock (Pietruszczak et al 1980). Most subsidence studies that include strain-soft-

ening do not provide details on how the softening was implemented (Mohammad et al 1998; Coulthard et al 2008; Esterhuizen et al 2010; Vakili et al 2010), which makes it difficult, if not impossible, to validate the findings of these studies. Further, implementation of strain-softening into numerical models has been reported to give rise to issues of numerical instability and sensitivity to mesh size (Pietruszczak et al 1981). In this paper, strain-softening will be implemented by reducing only the cohesion to zero as a function of plastic deviatoric strain *(ε_{pd})*.

2.4.3 Ubiquitous joint model

Some numerical modelling software packages include an in-built material model to represent a material with a high density of parallel joint surfaces. A typical example of such a material is sedimentary rock. The constitutive model allows for the stiffness of the material normal to the joint plane to reduce to zero when the stress normal to the joint becomes tensile. The ubiquitous joint material has been used to represent overburden strata in numerical models when predicting subsidence (Coulthard et al 1988; Coulthard et al 2008; Esterhuizen et al 2010).

2.4 Constitutive laws for caved goaf material

Limitations of some of the previous comparative studies of prediction of subsidence have typically left the extracted longwall panel as a void and as a result the numerical model would not have predicted vertical stress to be transmitted through the longwall floor. It is suggested that this is important for prediction of subsidence above multi-seam longwall panels.

The goaf initially is a pile of caved material that compacts as the overlying strata deflect and apply load to it. Results from field investigations show that there is significant variation in the heights of the caved goaf above the longwall floor. Many engineers estimate the height of the caved goaf above the longwall floor by assuming that the height of the caving is controlled by the bulking nature of the immediate roof of the longwall panel. The total height of the caved goaf above the longwall floor *(h_g)* can be approximated using Equation (1) if the convergence of the longwall roof and floor is much smaller than the extracted seam height *(T)*.

$$h_g = T\left(\frac{1}{b-1}+1\right) \qquad (1)$$

Although it has been claimed that the geology governs the degree of bulking of the caved goaf, there appear to be discrepancies concerning its relative effect. The bulking factor *(b)* is defined as the total bulked volume of the caved material divided by the original volume of the intact rock prior to bulking (Pappas et al 1993). It is equivalent to the void ratio plus 1. The values for bulking ratio presented in literature vary from 1.2 to 1.5 and are discussed in detail in Suchowerska (2014). This study shall consider a bulking factor of 1.2, as this is the magnitude typically used in numerical analyses with overburden strata consisting of sandstone.

Only a few field investigations have been conducted to measure the relationship between stress and strain of the caved goaf, and measurements show a definite trend of strain-hardening (Wardle et al 1983; Smart et al 1987; Trueman 1990). However, currently there is no preferred constitutive law that should be used for the caved goaf. The Terzaghi elastic strain-stiffening material model was used in this study, where the tangent Young's modulus *(E_t)* is defined as:

$$E_t = E_i + a\sigma \qquad (2)$$

Where E_i is the initial tangent modulus, σ is the applied uniaxial stress, and parameter a is a dimensionless constant. Derivation of the corresponding stress-strain relationship and secant modulus *(E_s)* for the caved goaf was detailed in the paper by Morsy and Peng (2002). There is limited information on the appropriate magnitudes for parameters a and E_i. Laboratory testing of caved goaf made from shales and sandstones gave a range of 10 – 15 for a and 5-6MPa for E_i (Pappas et al.1993). The magnitudes of parameters a and E_i , obtained from back analysis in a numerical model, were 355 and 31MPa respectively (Morsy et al 2002). These parameters used in the numerical model were selected to ensure that the magnitude of the virgin vertical stress was recovered in the centre of the longwall panel after extraction.

3. Problem Definition

The aim of this paper is to assess the effect of the material properties used to represent the overburden and the caved goaf of a longwall panel on the accuracy of the predicted final vertical subsidence of the ground surface when compared with field measurements. In particular, various constitutive laws are assessed on the basis of whether they can predict:

(i) a realistic subsidence profile; and

(ii)) that the vertical stress along the longwall floor returns to the overburden stress in the centre of the longwall panel.

The numerical model consists of a cross-section parallel to the longwall face and assumes plane-strain conditions. The initial pre-mining geometry of the model has an overburden depth *(H)* of 150m, the width of all the longwall panels *(W)* of 300m, interburden between the first and second seam *(B)* of 40m and the height of extraction in the first seam (T_1) and the second seam (T_2) of 3m (Figure 3(a)). The Young's Modulus for all of the coal measure strata was kept constant at $E = E_o = E_c$ = 10GPa. The bottom of the finite element mesh is fixed and normal displacements only are fixed on left and right boundaries.

Two different models are considered to represent the post mining strata upon extraction of the longwall panel in the first seam: Seam1-Cavity model and Seam1-Goaf model. The Seam1-Cavity model assumes that the cavity generated by the extraction of the coal seam can be left as a void, as shown in Figure 3(b). Although leaving the void created by the extracted longwall panel as a cavity may not be realistic, this model provides a lot of detailed information on how the overburden behaves, which might otherwise be masked. The Seam1-Goaf model assumes that a strain-stiffening material can be used to represent the behaviour of the caved goaf. The caved goaf represents the roof of the longwall panel that has collapsed onto the longwall floor and bulked in volume so as to fill the void left by the extracted coal. The geometry of the Seam1-Goaf model is shown in Figure 3(c).

Two models are also considered for the second seam longwall extraction: Seam2-Stacked model and Seam2-Staggered model. The panels in both

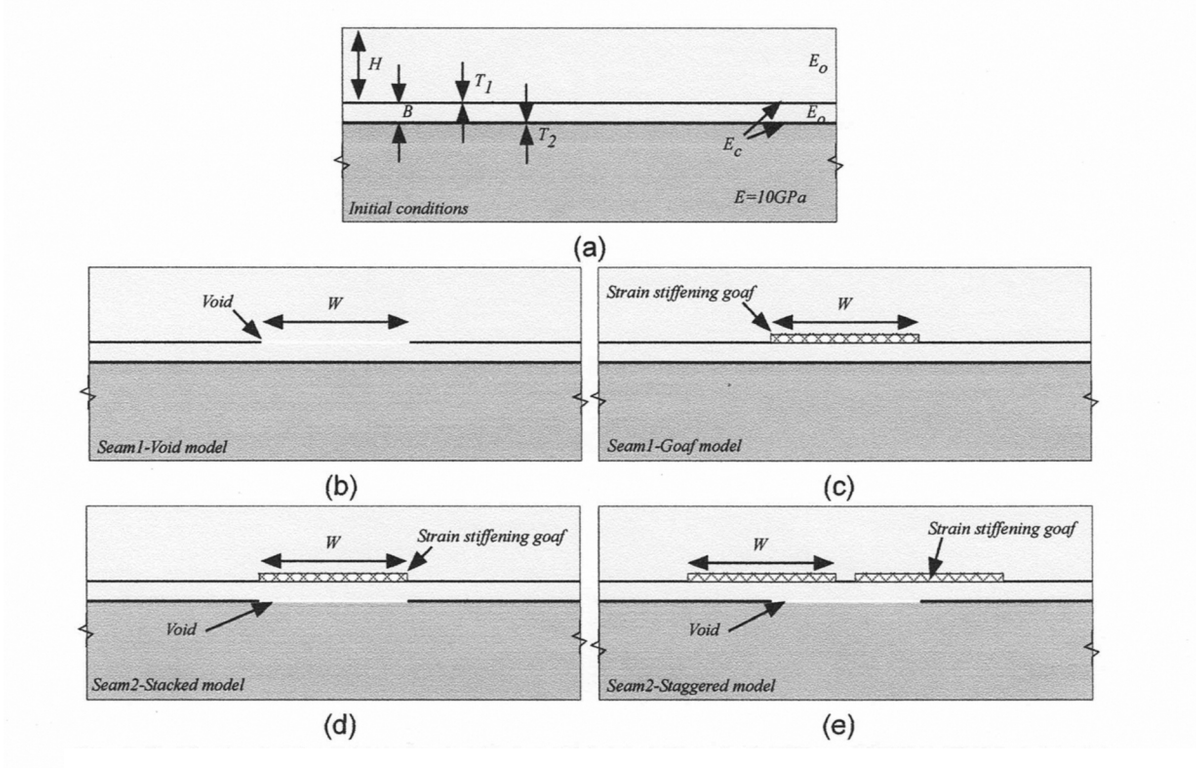

Figure 3 **Scale drawing of geometry and material properties of: (a) initial conditions of all models, (b) Seam1-Cavity model, (c) Seam1- Goaf model, (d) Seam2-Stacked model and (e) Seam2-Staggered model**

seams are assumed to be parallel. In the Seam2-Stacked model, the longwall panel extracted in the first seam lies directly above the longwall panel extracted in the second seam (Figure 3(d)). In the Seam2-Staggered model, two longwall panels are extracted in the first seam and one longwall panel extracted in the second seam. The centreline of the longwall in the second seam aligns with the centre of the chain pillar in the overlying seam (Figure 3(e)). The models assume that the caved goaf created upon the extraction of a longwall panel in the first seam is represented as a strain-stiffening material. The longwall panel in the second seam is left as a void to provide detailed information on how the overburden and interburden behave, which might otherwise be masked.

3.1 Constitutive laws for caved goaf

The constitutive laws for the caved goaf were implemented in the commercial finite element program ABAQUS through a Fortran script. This script adopted Equation (2) to update the Young's modulus of the material as a function of the total vertical strain. The vertical strain was used in this instance as the constitutive law was originally designed for 1D conditions. The script did not allow the newly calculated Young's modulus to exceed the original Young's modulus of the overburden strata. For the strain-stiffening goaf, the bulking factor is assumed to be equal to a magnitude of 1.2, such that the height of the caved goaf is equal to six times the extracted height above the longwall floor (i.e. 18m). The strain-stiffening constitutive law proposed by Terzaghi is used to represent the behaviour of the caved goaf. Three degrees of stiffening were used for Terzaghi strain-stiffening caved material in the Seam1 models and they have been labelled as Soft, Average and Stiff. The magnitude of the parameters for the three degrees of stiffness is defined in Table 1.

For the Seam2 models, efforts were made to narrow the range of possible magnitudes of parameters a and E_i by assuming that the strain-stiffening goaf material could possibly return to its original stiffness when the overburden stress is achieved in the goaf. Therefore, the upper limit of the magnitude of strain can be associated (at least approximately) with the displacement required for the goaf material to return to a state of zero air voids. In principle, a state of zero air voids would occur when the particles in the bulked material rearrange and compact such that no voids are left in the material. Considering one-dimensional deformation, the vertical strain required for the caved goaf material to return to a state of zero air voids would correspond to a magnitude of b-1. Therefore the upper limit of the stress strain curve would correspond to a vertical stress given by

$$\sigma = \frac{E_i}{a}\left(e^{\varepsilon a} - 1\right) = \frac{E_i}{a}\left(e^{a(b-1)} - 1\right) \qquad (3)$$

Once the strain-stiffening goaf reaches a state of zero air voids, the behaviour of the reconstituted goaf material can be assumed to return back to its original elastic behaviour with Young's modulus defined as E_o. On this basis, it can be assumed that the Young's modulus of the strain-stiffening elastic material is equal to E_o when $\varepsilon = b$-1. Therefore, by differentiation of Equation (3) the tangent modulus of the strain-stiffening material for a given strain can be determined, as given by

$$\frac{d\sigma}{d\varepsilon} = E_i e^{a\varepsilon} \qquad (4)$$

When the gradient of the stress strain curve of the strain-stiffening material is equal to E_o and $\varepsilon = b$-1, then the parameters for a and Ei become mutually dependent, as given in Equation (5)

$$a = \frac{1}{b-1} ln\left(\frac{E_0}{E_i}\right) \qquad (5)$$

Name of goaf material	E_i	a	Reference
Stiff	30,000kPa	350	Based on numerical work by Morsy and Peng (2002)
Average	20,000kPa	50	
Soft	5,000kPa	15	Based on experimental work by Pappas and Mark (1993)

Table 1 Definition of parameters used for the Terzaghi strain-stiffening material

A bulking factor (b) of 1.2 is also assumed for the caved goaf material in the Seam2 models. E_i = 5MPa is assumed and together with E_O = 10GPa and b = 1.2 give a = 38, according to Equation (5).

3.1.1. Constitutive laws for coal measure strata

The overburden above the longwall panel is considered as three mechanically different materials: an isotropic linear-elastic material, an elastoplastic material and a jointed material. Table 2 specifies all the parameters used in the reference case and parameters considered for the overburden in the Seam1 models. The initial stress state was assumed to have a ratio of horizontal to vertical stress of 1.5. This will be significant in non-linear analyses. The effects of overburden stiffness (E_o) and caved goaf stiffness for an overburden defined as an isotropic linear-elastic overburden were assessed.

An elastic-perfectly plastic and an elastoplastic strain-softening material are considered. The Mohr-Coulomb criterion with φ = 30 degrees was used as it was found to give best agreement between the predicted ratio $(W/H)_{crit}$ and what is typically recorded in the field (Suchowerska 2014). The magnitude of cohesion was selected to be low enough to ensure the overburden would fail. Although the magnitudes considered may seem larger than the typical measured strength of discontinuities or smaller than the typical measured strength of intact coal measure rocks, it is necessary to remember that this magnitude of cohesion is representative of the smeared coal measure strata, including all defects. Although this magnitude selected may not always reflect a realistic value for the smeared coal measure strata, the analyses here were conducted primarily to obtain an indication of the overall behaviour of an elastic-perfectly plastic material. The rate of softening for the elastoplastic strain-softening material was defined using the plastic deviatoric strain (ε_{pd_max}), by which point the cohesion would have been reduced to zero. The ratio of c to $\varepsilon_{pd_max}$was kept constant at 10,000kPa.

Bedding planes typically found in coal measure strata were represented by three different forms of constitutive laws: a transversely isotropic elastic material, a ubiquitous joint material and an isotropic elastic material with smooth interfaces at the horizontal strata boundaries. The bedding planes were assumed to lie horizontally in the overburden material. The transversely isotropic elastic material was implemented by specifying a value of the independent shear modulus (G'). The independent shear modulus in Table 2 has been normalised by the isotropic elastic shear modulus defined by $G_{iso}= E/2(1+\nu)$, where ν is the Poisson's ratio and was assumed to equal 0.25.

The ubiquitous joint material obeys pre-defined constitutive laws incorporated in the ABAQUS software. This constitutive model assumes that the material can fail by either slipping along a set of parallel surfaces or as a bulk material, as discussed earlier in this paper. The ubiquitous horizontal joints are defined by a joint friction angle φ = 30 degrees, joint cohesion c = 0kPa, and an associated flow rule.

Incorporation of smooth interfaces into the isotropic elastic overburden, referred to in this paper as a bedded material, would allow the over-

Table 2 - Variable definition and values used in parametric study.

Variable	Definition	Values used in reference case	Values considered
E_o	Young's modulus of overburden	10GPa	5, 1GPa
c	Cohesion of overburden	-	1500, 2000, 2500kPa
G'/G_{iso}	Norm. independent shear modulus	1.0	0.334, 0.167, 0.1
D	Spacing of bedding planes	No bedding	30, 15, 7.5m

Table 2 Variable definitions and values used in parametric study

burden to shear and slide in the horizontal plane more easily than for an isotropic elastic overburden. The smooth interfaces are positioned at a vertical spacing of *D* through the whole depth of the overburden. Although in reality the properties of the bedding planes are not perfectly smooth, this study considers the effect of the most conservative of conditions.

4. Results

The results are presented according to the three forms of constitutive laws used to represent the overburden and interburden. Results are presented for the subsidence, sub-surface strata displacement and stress redistribution. Although there have been many reviews of the predictions of subsidence using an isotropic elastic overburden, it is included here for completeness and is used when comparing results obtained using numerically expensive constitutive laws. More detailed information about the results from the study are detailed in Suchowerska (2014).

4.1 Single-seam longwall panels

When the overburden was represented as an isotropic linear-elastic material in the Seam1-Void model, the predicted subsidence profile is shallower and wider than what is normally observed in the coalfields of NSW. This agrees with the findings presented by previous authors (Coulthard et al 1988; Kay et al 1991). The magnitude of S_{max} is proportional to Young's modulus *(E)*, while the ratio S_{edge}/S_{max} for all magnitudes of E remains constant at 47%. Plots of principal stress show that the overburden above the first extracted longwall behaves similarly to a simply supported beam. Bridging actively redistributes all the vertical load of the unsupported overburden to the remaining coal pillars on either side of the longwall. This induces very high vertical stresses into the adjacent coal pillars. This vertical stress increase in the coal pillars is significantly greater than those calculated from analytical calculations or stress measurements recorded in the field.

Figure 4 shows the subsidence profiles obtained from the four material combinations considered in the Seam1-Goaf model. A Stiff Goaf and Soft Goaf stiffness were used for the Terzaghi strain-stiffening caved goaf material (Table 1) and two

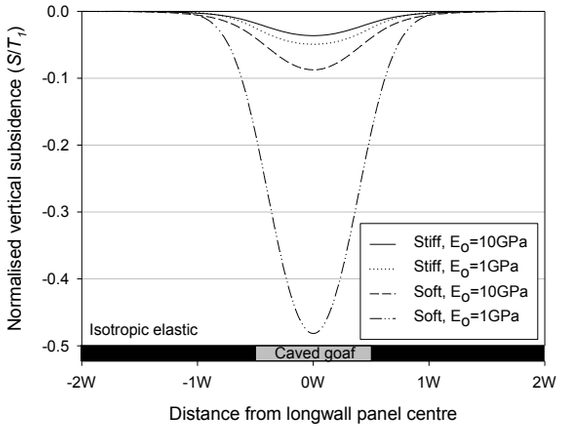

Figure 4 **Results of normalised surface vertical displacement from the Seam1-Goaf model with varying Young's modulus of the elastic overburden *(E_o)* and goaf material**

magnitudes of E_o were used for the overburden strata (i.e., 1GPa and 10GPa). The maximum subsidence *(S_{max1})* for both cases with Stiff Goaf is approximately 4% of T_1. The maximum subsidence *(S_{max1})* for cases with Soft Goaf is approximately 8% and 50% of T_1 for the Eo= 10GPa and E_o= 1GPa, respectively. The Soft Goaf with the softer overburden achieved a maximum subsidence closest to what is typically observed in the field (i.e. 60% of T_1). The ratio S_{edge}/S_{max} for all four goaf cases all fall in the range of approximately 50-60%. This result continues the trend that isotropic linear-elastic overburdens overestimate the relative subsidence above the edge of the longwall panel relative to the maximum subsidence.

Figure 5 (pxx) shows the vertical stress at the height of longwall floor for all four material combinations considered in the Seam1-Goaf model. The vertical stress in the caved goaf returns to the original in situ stress only when E_o = 1GPa and the Stiff Goaf is used. The cases with the Stiff Goaf led to the larger magnitude of vertical stress in the centre of the panel. Wilson's equation for the vertical stress on the longwall floor (Wilson 1980) has been plotted in Figure 5 for an abutment angle *(β)* of 21 degrees. This magnitude of abutment angle was chosen as a reference according to the recommendations made by Colwell (1998). The combination of the Stiff Goaf and E_o = 1GPa best matches Wilson's (1980) equation.

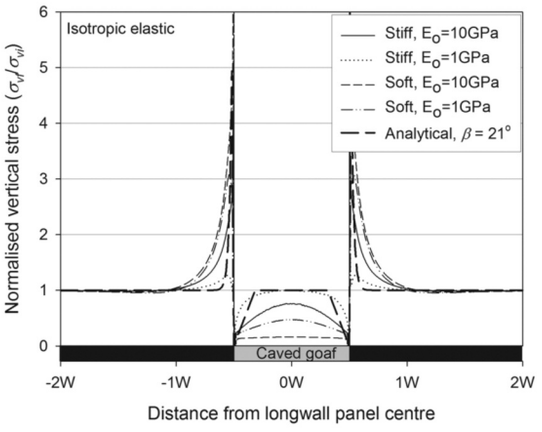

Figure 5 **Results of normalised vertical stress at the height of the longwall floor from the Seam1-Goaf model with varying Terzaghi strain-stiffening material and Young's modulus of the elastic overburden *(E_o)* together with Wilson's analytical vertical stress distribution**

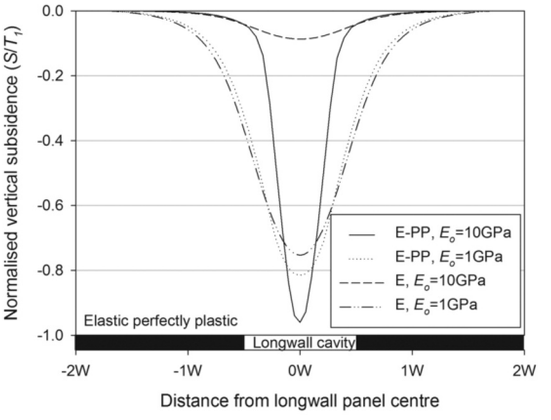

Figure 6 **Results of normalised vertical subsidence from the Seam1-Cavity model with varying Young's modulus for an elastic-perfectly plastic overburden (E-PP) and elastic overburden (E)**

In general, the addition of the strain-stiffening goaf to the numerical model responded effectively like adding springs between the longwall roof and the longwall floor. Therefore, the stress transmitted onto the longwall floor appears to be governed by the relationship of relative stiffness of the overburden to the caved goaf material. The principal stress plots show that if the overburden is relatively stiff and the goaf is relatively soft, the overburden effectively bridges its entire vertical load to the surrounding strata. If the overburden and goaf are either both relatively stiff or both relatively soft, the goaf attracts some vertical stress but it does not return to the original overburden stress level. If the goaf is relatively stiff and the overburden relatively soft, the vertical stress in the goaf returns to the original overburden stress along the longwall floor. These results are as expected of an elastic analysis where generally stiffer elastic materials attract greater stress than less stiff materials.

Elastoplastic overburden

Figure 6 presents the predicted subsidence for the Seam1-Cavity model for two magnitudes of E_o, when the overburden material is defined as an elastic-perfectly plastic material. Failure in the overburden is defined by the Mohr-Coulomb failure criterion with c = 2000kPa and φ = 30 degrees. Unlike the elastic overburden, the shape of the elastic-perfectly plastic subsidence profile is different for the two magnitudes of E_o. The normalized maximum vertical subsidence is 96% and 82% of T for E_o = 10GPa and E_o = 1GPa, respectively. The magnitude of ratio S_{edge}/S_{max} is 5% and 45% for E_o = 10GPa and E_o = 1GPa, respectively. In an elastic analysis this would be counter-intuitive, but this is no longer the case when plasticity governs the deformations of the overburden. It should be noted, that even though the vertical subsidence is less than the full extracted seam height *(T_1)* in both these cases, the roof and floor of the longwall come into contact because of compression of the coal seam from the abutment loads and some floor heave. The significantly different shapes of the two subsidence profiles arise from the softer overburden sagging more prior to the onset of failure than the stiffer overburden. This can be better appreciated by comparing the subsidence for the elastic-perfectly plastic overburden to the isotropic linear-elastic overburden results (also shown in Figure 6). The softer overburden underwent much less plastic straining before the longwall roof touched the longwall floor and further vertical displacements ceased, than for the stiffer overburden.

Distributions of the vertical displacement for the elastic-perfectly plastic overburden show that there is a mass downward movement of a trapezium-shaped block of the overburden directly

above the extracted longwall panel. This failure mechanism has previously been described as Terzaghi's trap door problem. The overall shape of the subsidence curves (Figure 6) appear to be primarily governed by the elastic properties of the overburden outside the area of failure, and by the plastic flow rule along the failure surface for the trapezium-shaped block of overburden. For this reason, the subsidence bowl is still relatively wide for the case where E_o = 1GPa.

The plots of principal stress for the elastic-perfectly plastic overburden show that, even though the roof comes into contact with the floor of the longwall, the overburden bridges a lot of the vertical stress to the remaining coal pillars. This occurs because a yielded elastic-perfectly plastic material is still able to support stresses that caused it initially to fail. Even after yielding the overburden will continue to bridge the same vertical load to the surrounding strata that it was transmitting at the onset of failure. Therefore, the principal stress plot for an elastic-perfectly plastic overburden is somewhat similar to the principal stress plot for an isotropic linear-elastic overburden. As such, the predictions of subsidence using the Seam1-Goaf model with an elastic-perfectly plastic overburden did not return the magnitude of the vertical stress on the longwall floor to the original overburden stress.

Figure 7 presents the subsidence profile for the Seam1-Goaf model with the elastoplastic strain-softening overburden for the Average Goaf. For the other caved goaf stiffnesses that were considered, the Stiff Goaf did not allow for the overburden to yield and it was not possible to find a stable solution for the Soft Goaf. The solution was noted to vary for other magnitudes of horizontal in situ stress to vertical in situ stress *(K)*. The results show that smaller magnitudes of cohesive strength of the elastoplastic strain-softening overburden increase the predicted maximum subsidence. The strain-softening material also changes the general shape of the subsidence profile. The ratio S_{edge}/S_{max} reduces from 48% for an elastic overburden with an Average Goaf to 19% for the elastoplastic strain-softening overburden with c = 1500kPa and $\varepsilon_{pd\_max} = 0.15$ (Figure 7).

The vertical stress at the elevation of the longwall floor for the Seam1-Goaf model with an elastoplastic strain-softening overburden is presented in Figure 8. Unlike an isotropic linear-elastic overburden or an elastic-perfectly plastic overburden, the elastoplastic strain-softening material's response to a reduction in overburden strength increases both the subsidence and the maximum stress induced into the caved goaf. This relationship arises because of the very essence of the strain-softening material, where the initial stresses that induced failure need to then redistribute as a result of a reduction in strength with plastic strain-

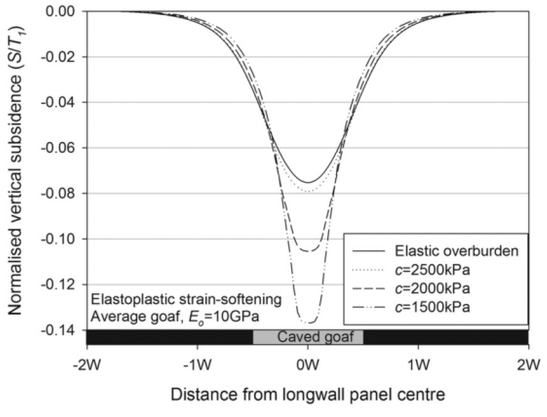

Figure 7 **Plot of normalised vertical subsidence from the Seam1-Goaf model for the average goaf and elastoplastic strain-softening overburden with E_o=10GPa and varying maximum cohesion**

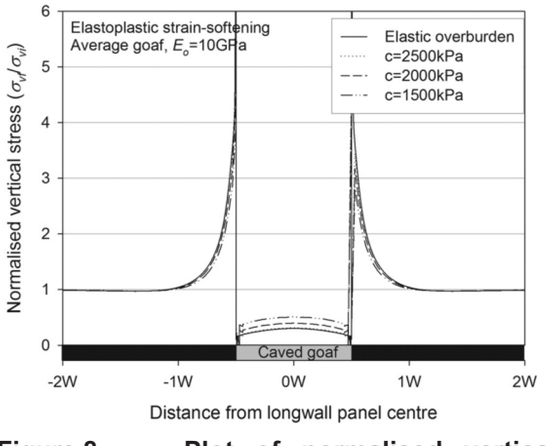

Figure 8 **Plot of normalised vertical stress at the height of the longwall floor from the Seam1-Goaf model for the average goaf with elastic and elastoplastic strain-softening overburden with E_o=10GPa and varying cohesion *c*.**

ing. It should be noted that the solution to the problem being analysed often ran into numerical instabilities and was also sensitive to mesh size (Pietruszczak et al., 1981). A more robust implementation of strain-softening constitutive laws in FEM is required before its potential in prediction of subsidence can be rigorously assessed.

Bedded overburden

Transversely isotropic elastic overburden in the Seam1-Cavity model predicts deeper subsidence profiles than the isotropic elastic case, while the magnitudes of subsidence above the edge of the longwall panel remained relatively constant. This leads to a reduction in ratio S_{edge}/S_{max} for increased anisotropy. The transversely isotropic elastic overburden gives rise to a subsidence profile closer to what is typically recorded in the field, as previously noted by other authors (Wardle et al 1983; Coulthard et al 1988; Kay et al 1991). However, a transversely isotropic elastic overburden did not affect the predicted stress redistribution in the overburden. For all degrees of anisotropy the stress distribution in the overburden was similar to what is predicted for an isotropic linear-elastic overburden. Therefore, the use of transverse isotropy in the overburden material may lead to prediction of more accurate subsidence profiles for single-seam subsidence, but it would probably not be suitable for subsidence prediction above multi-seam longwall panels, as the vertical stress is unlikely to transfer through the goaf and onto the interburden.

Figure 9 shows the subsidence profiles from the Seam1-Goaf model where overburden is defined by the ubiquitous joint material with E_o= 10GPa and E_o= 1GPa. Numerical instability prevented a solution for the Seam1-Goaf model with a Soft Goaf to be found. All the overburdens yielded by slipping along the horizontal ubiquitous joints except for the case with a Stiff Goaf and E_o= 1GPa. The Stiff Goaf provided support for the overburden so that it did not deflect and yield. The effect of the overburden slipping along the ubiquitous joints on the subsidence profile is quite evident. There is a significant increase in the maximum predicted subsidence.

There are several similarities in the results obtained from the ubiquitous joint material to those obtained from the elastic-perfectly plastic overburden. The ubiquitous joint material predicts a mass downward movement of a trapezium-shaped block of the overburden similar in shape to that which forms in the elastic-perfectly plastic overburden. However, the ubiquitous joint material does not bridge as much stress to the

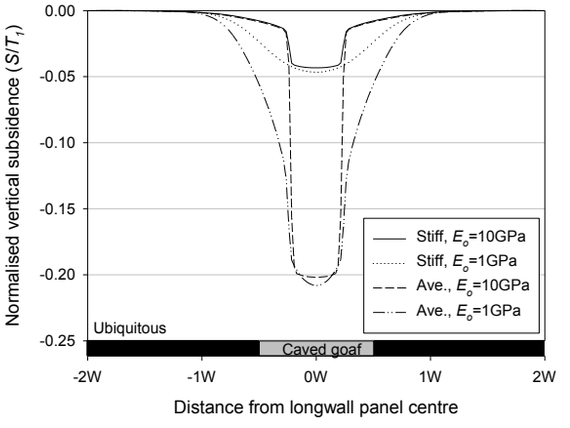

Figure 9 **Plots of surface vertical displacement normalised by extracted seam height for the Seam1-Goaf model with a ubiquitous jointed overburden material**

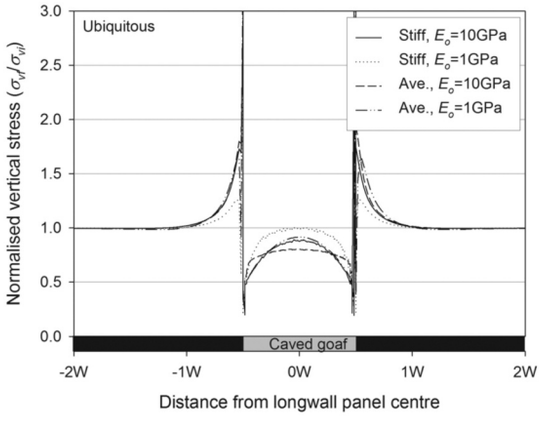

Figure 10 **Plots of normalised vertical stress at the height of the longwall floor from the Seam1-Goaf model with a ubiquitous jointed material overburden**

surrounding strata and allows it to transfer into the goaf. Figure 10 shows the predicted vertical stress distribution on the longwall floor for all four cases considered of the ubiquitous joint material in the Seam1-Goaf model. The Stiff Goaf and E_o= 1GPa predict a return to overburden stress, while the other three cases all predict a maximum vertical stress of at least 80% of overburden stress.

Figure 11 shows the subsidence profiles from the Seam1-Cavity model where smooth interfaces are included in an isotropic linear-elastic overburden, with E_o = 10GPa. The interfaces are separated by a distance D starting at the top surface of the model. Including smooth interfaces in the overburden increases the maximum subsidence (S_{max}) and also changes the shape of the subsidence profile. Smooth interfaces spaced at intervals of 15m or less allows the cavity roof to touch the floor of the longwall panel and the subsidence to reach 100% of T. The subsidence at the panel edge (S_{edge}/S_{max}) reduces from 47% for the isotropic elastic overburden down to 1% for the elastic overburden with smooth interfaces spaced at 7.5m intervals.

The results from the elastic overburden with smooth interfaces have shown that the layer thickness needs to be thin to achieve a desired flexibility in the overburden to be able to predict the desired magnitude of maximum subsidence above the longwall panel. The principal stresses predicted for the elastic overburden with smooth interfaces show that each layer of the overburden behaves as described for the case of a homogeneous elastic overburden, i.e. as a simply supported beam. The roof and floor of the cavity only come into contact when 15m and 7.5m thick elastic layers are used for the overburden. The area of roof and floor in contact is smaller for the 15m thick layers than for the 7.5m layers, and consequently the stress on the longwall floor is more concentrated (Figure 12). Therefore, an

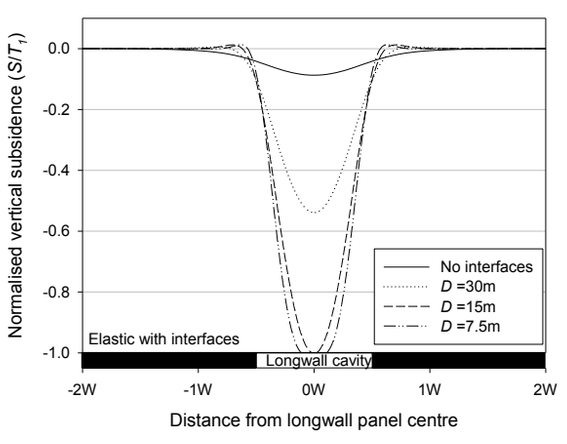

Figure 11 **Plots of vertical subsidence normalised by extracted seam height for the Seam1-Cavity model with an elastic overburden material and smooth interfaces separated by spacing D**

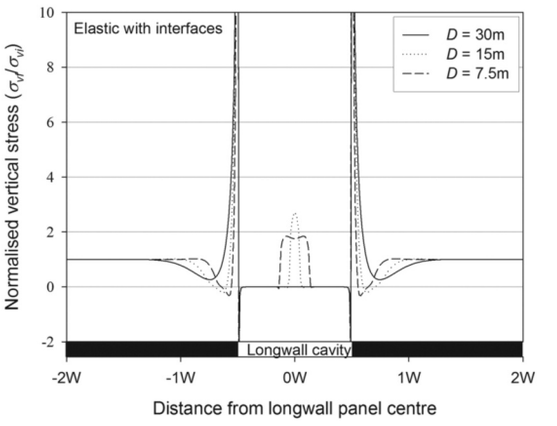

Figure 12 **Plots of normalised vertical stress at the height of the longwall floor from the Seam1-Cavity model with an elastic overburden material and smooth interfaces separated by spacing D**

overburden composed of this bedded material also leads to less overburden load being transferred to the surrounding strata and more onto the longwall floor.

The results presented in Figure 13 are for the Seam1-Goaf model with an elastic overburden with smooth interfaces spaced every 7.5m. Three degrees of stiffness are considered for the strain-stiffening material, where the strain-stiffening parameters are provided in Table 1. The stiffness of the strain-stiffening goaf material appears to govern the maximum subsidence. This leads to the Soft

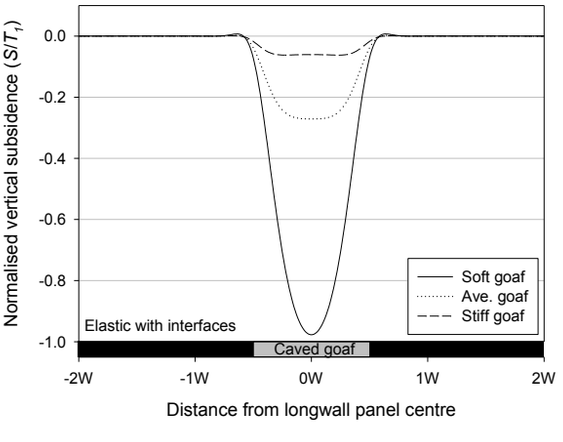

Figure 13 **Plots of surface vertical displacement normalised by extracted seam height for the Seam1-Goaf model with an elastic overburden material and smooth interfaces spaced every 7.5m**

Goaf predicting the maximum subsidence of almost the full extracted seam height. The Average Goaf and Stiff Goaf predict a maximum subsidence of 27% and 6% of T respectively. The selection of appropriate magnitudes of strain-stiffening goaf parameters would need to be further investigated, possibly through back calculation, to achieve a prediction of maximum subsidence equal to the magnitudes typically recorded in the field.

Figure 14 presents the vertical stress along the longwall floor for the three degrees of goaf stiffness and an elastic overburden with smooth interfaces spaced every 7.5m. All three degrees of goaf stiffness predict a return to overburden stress in the middle of the longwall panel. The stiff goaf predicts the widest width of the longwall floor to return to the overburden stress.

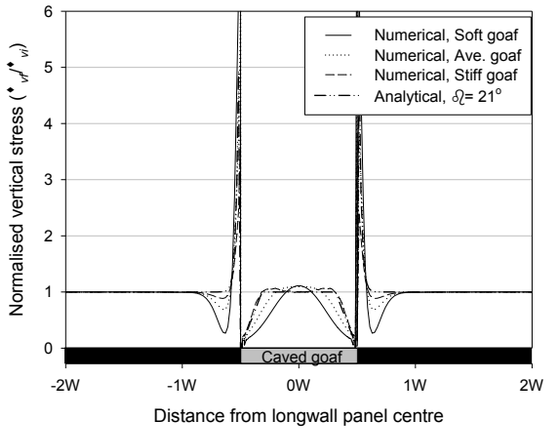

Figure 14 **Plots of normalised vertical stress at the height of the longwall floor from the Seam1-Goaf model with an elastic overburden material and smooth interfaces spaced every 7.5m**

4.2 Multi-seam longwall mining

To accurately predict multi-seam subsidence, the material models used for the overburden would need to ensure an appropriate subsidence bowl shape is obtained as well as allowing for the load of the overburden to be transferred through the first seam goaf and onto the interburden. The findings obtained from the analyses presented above suggest that this could possibly be achieved by using a strain-stiffening caved goaf material in the first seam with a strain-softening overburden, a ubiquitously jointed overburden or with an elastic overburden with closely spaced smooth interfaces. The strain-softening material and ubiquitously jointed material were found to be more numerical taxing and led to more numerical instabilities. Therefore, in this paper, only the elastic material with closely spaced smooth interfaces is considered.

Figure 15 shows the predicted incremental subsidence after the extraction of each longwall panel in the Seam2-Stacked model when the bedded material was used to represent the overburden and interburden and derived goaf parameters of E_i=5MPa and a = 38 were used. The maximum subsidence above the longwall panel in the first seam was 47% of T_1. As previously noted, the stiffness of the caved goaf material controls the magnitude of maximum subsidence above the first seam. The maximum incremental subsidence upon extraction of the second seam was 103% of T_2. The incremental subsidence profile for the second seam is primarily contained within the width of the longwall panel. The incremental subsidence for the second seam is larger than the extracted thickness of the second seam because the strain-stiffening caved goaf has undergone additional compaction. This has occurred because the vertical stress in the caved goaf material of the first seam increases when upon extraction of the second seam the stress is redistributed.

Contour plots of vertical stress within the subsurface strata show that the bedded overburden

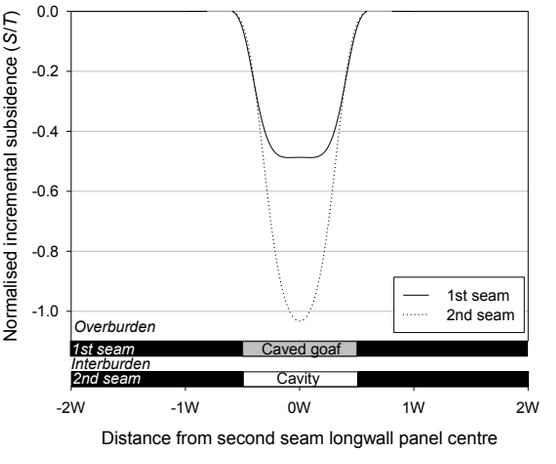

Figure 15 **Plot of incremental subsidence profiles from the stacked arrangement after extraction of the longwall in the first seam and the second seam with a bedded overburden**

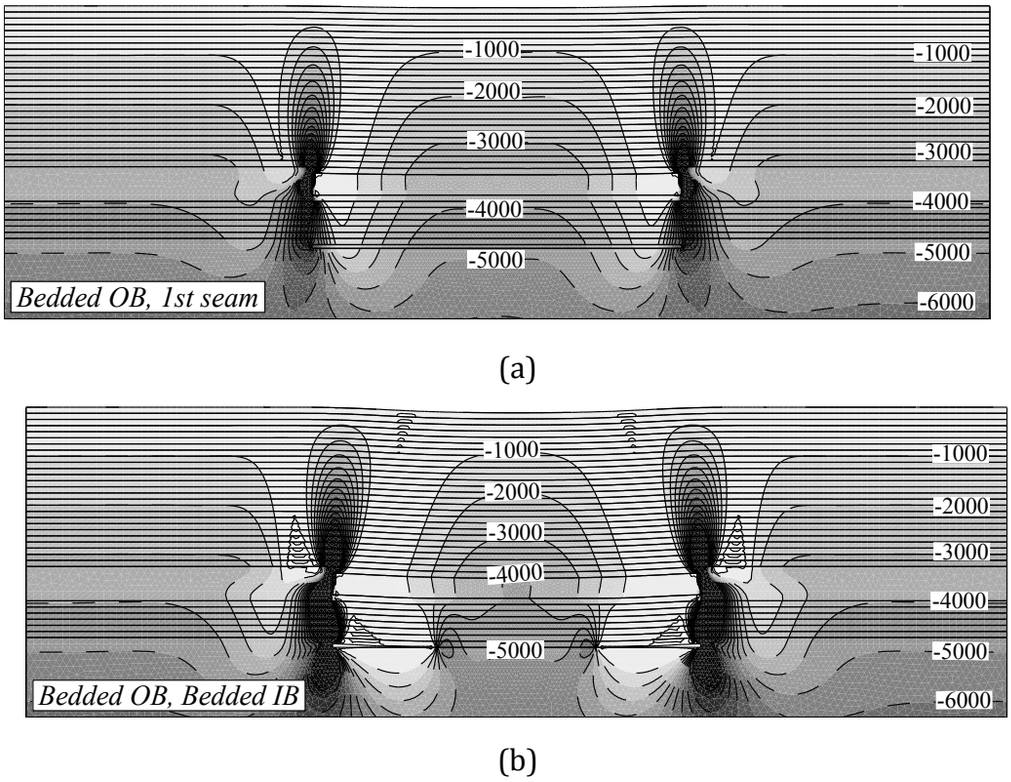

Figure 16 **Plots of vertical stress in kPa for the stacked arrangement with bedded interburden and overburden:**
(a) after extraction of the first seam longwall
(b) after extraction of the second seam longwall

allows the stress in the caved goaf to return to the same magnitude as the initial overburden stress after the extraction of the longwall in the first seam (Figure 16(a)). Since the layer thickness is small enough in the overburden and the interburden, generally the vertical stress is equal to the original overburden stress. Upon extraction of the second seam a similar vertical stress distribution was observed in both the first seam and the second seam, whereby the original overburden stress is achieved in the centre of the longwall panels with a reduction to zero vertical stress at the rib-edges of the longwall panels (Figure 16(b)).

Figure 17 shows the predicted incremental subsidence after extraction of the longwall panels in both seams from the staggered arrangement with a bedded overburden and interburden. The maximum subsidence for the first seam longwalls was 49% of T_1. The subsidence profile above longwalls in the first seam appears to consist of the superposition of two incremental subsidence profiles predicted using a bedded overburden. This superposition does not result in significant overall subsidence above the chain pillar. This is because the sagging of the bedded overburden strata is limited primarily to the width of each individual longwall panel. The maximum incremental subsidence induced by extracting the longwall in the second seam is 100% of T_2.

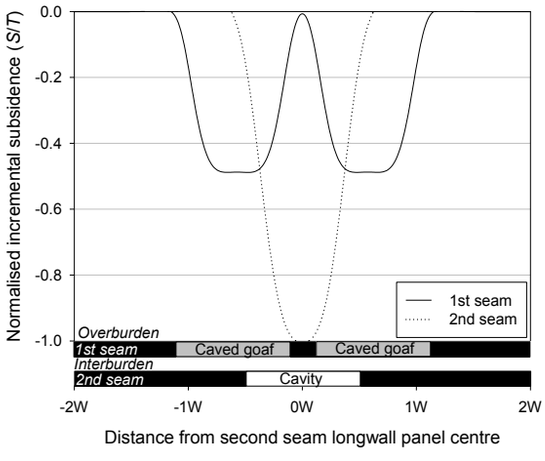

Figure 17 **Plot of incremental subsidence profiles from the staggered arrangement after extraction of the longwalls in the first seam and the second seam with a bedded overburden**

Contour plots of the vertical displacement for the staggered arrangement with a bedded overburden showed very similar mechanics as was noted for the stacked arrangement. The displacement of the bedded overburden after extraction of the longwall panels in the first seam causes a sagging of the overlying strata. Significant displacements only occur in the strata directly above the extracted longwall panel, and do not extend past the rib-edges. This response is also observed in the second seam with some minor lateral spreading of vertical displacements through the strain-stiffening goaf material in the first seam.

5. Discussion

The material models used for the overburden in this paper have yielded a wide range of predicted subsidence shapes and distributions of vertical stress on the longwall floor. Considering only the subsidence results above the extraction of the first seam, some general observations can be made about the advantages and limitations of certain constitutive laws. As has been previously documented, in general, isotropic elastic overburdens predict wider and shallower subsidence profiles than that which is recorded in the field (Fitzpatrick et al 1986; Coulthard et al 1988).

Using an elastic strain-stiffening material to represent the caved goaf can control the sag of the overburden and ultimately the magnitude of the maximum subsidence. Both the elastic-perfectly plastic and the ubiquitous joint material give rise to a sudden increase in magnitude of subsidence that occurs above the yielded zone. The transversely isotropic material and the elastic material with smooth interfaces show the best agreement with subsidence measurements made in the field. Therefore, if a numerical model need only to predict accurately the shape and magnitude of a single-seam subsidence profile, the findings from this paper would imply that a transversely isotropic elastic or an elastic material with closely spaced interfaces would probably be the best possible materials to use for the overburden. Both of these material models are not very taxing numerically.

The Seam1-Goaf model successfully allowed for some of the load of the overburden to be transferred onto the longwall floor. In general, less stress was induced into the caved goaf material when there was a larger difference between the relative stiffness of the caved goaf material and the relative stiffness of the overburden material. Also, in general, if the overburden was allowed to yield (i.e. in the cases where the overburden was elastic-perfectly plastic, elastoplastic strain-softening or a ubiquitous joint material) there was more stress induced into the goaf than for equivalent caved goaf stiffness and non-yielding overburden material. The exception was the isotropic elastic overburden with closely spaced smooth interfaces. If a numerical model needs only to predict accurately the magnitude of vertical stress on the longwall floor, the findings would imply that a relatively stiff elastic strain-stiffening caved goaf material with a relatively soft overburden would be the best possible material combination. However, the effect of the yielding nature of the coal seam, longwall roof and longwall floor would need to be further investigated.

A culmination of the findings from the prediction of subsidence above a single seam longwall panel led to the conclusion that the elastic material with closely spaced smooth interfaces would be the most appropriate material to use in prediction of subsidence above multi-seam longwall panels. This is because it would be able to predict a reasonable shape for the subsidence profile and allow for the load of the overburden to be transferred through the first seam goaf and onto the interburden. The strain-softening material and ubiquitous material could also possibly be able to achieve this, however they were not considered as they were more numerically taxing and led to many numerical instabilities.

The maximum subsidence was less than the 60% of T_1 typically observed in the field for the first seam extraction in the multi-seam cases considered here. This can be modified in future studies by changing the magnitude of E_i and a, in keeping with the derived equation given in Equation (5). It should be noted that the stress achieved in the strain-stiffening material in the analyses was much less than is required to return the goaf to the original overburden stiffness (E_o). For the values of strain-stiffening parameters used in the multi-seam cases in this paper, of E_i = 5MPa and a =38, the stress required to reach a state of zero air void is

263MPa. The maximum stress achieved in the strain-stiffening caved goaf material was in the order of only 4MPa.

The displacement-finite element method (DFEM) was able to predict reasonably well the basic subsidence trough created above single-seam and multi-seam longwall panels. However, the DFEM was not successful in predicting the variations of subsidence above chain pillars in the first seam. If, as proposed by previous authors (Bai et al 1995; Gale 2004; Mine Subsidence Engineering Consultants 2007), the source of this local variation in subsidence is due to rearrangement of caved goaf material in the first seam further investigations should be conducted to identify if other numerical methods would be able to match the location variations in maxima and minima in the measured subsidence above multi-seam longwall panels.

The discrete element method might seem the most appropriate method to consider first, however, it should be noted that a reasonable representation of the stratigraphy and discontinuities around the first seam longwall would be required to achieve a plausible solution. A reasonable level of detail about the stratigraphy and discontinuities is often difficult to obtain for most real-life cases.

6. Conclusion

The predictions of vertical subsidence profiles above single-seam and multi-seam longwall panels were compared with measurements typically observed in coalfields in New South Wales, Australia. A selection of constitutive laws was used to represent the mechanical behaviour of the coal measure strata, varying in complexity from simple (e.g., an isotropic linear-elastic material) to very sophisticated (e.g., strain-softening elastoplastic material). A strain-stiffening goaf was also included in some models to allow for the generation of vertical stress on the longwall floor, and subsequently onto the interburden, in some cases allowing it to return to the original overburden stress.

The best agreement between the measured single-seam and multi-seam subsidence data was achieved by using a strain stiffening caved goaf material with the overburden and interburden defined as an elastic material with closely spaced frictionless horizontal interfaces.

The results show that more sophisticated and numerically taxing constitutive laws do not necessarily lead to more accurate results when the predictions are compared to field measurements. The two material models that included softening after the onset of yield (i.e. elastoplastic strain-softening and the ubiquitous joint materials) would also be able to achieve a predicted subsidence close to the field measurements, however, these computations are significantly more numerically taxing and the solution can be plagued with numerical instability. The transversely isotropic material and the elastic-perfectly plastic material would possibly be able to predict the shape of the subsidence profile reasonably well. However, these materials were not able to predict the return of overburden stress along the longwall floor because the overburden load is bridged to the surrounding strata.

An isotropic linear-elastic overburden is not able to match either the shape of the subsidence profile or the vertical stress distribution along the longwall floor. The displacement finite element method was not able to predict the variation in the subsidence profile local to the chain pillar in the first seam, because it was not able to replicate the remobilisation and compaction of the first seam goaf.

9. References

Bai M and Kendorski FS 1995 ‘Chinese and North American high-extraction underground coal mining strata behaviour and water protection experience and guidelines’, Proceedings of the 14th International Conference of Ground Control in Mining, Morgantown, WV, pp209-217

Colwell MG 1998 Chain Pillar Design (Calibration of ALPS) C6036, Australian Coal Association Research Program

Coulthard MA and Dutton AJ 1988 ‘Numerical modelling of subsidence induced by underground coal mining’ in Proceedings of the 26th US Symposium: Key Questions in Rock Mechanics, University of Minnesota, Minneapolis, Balkema, Rotterdam

Coulthard MA and Holt GE 2008 'Numerical modelling of mining near and beneath tailings dam', Southern Hemisphere International Rock Mechanics Symposium, Perth, Australian Centre for Geomechanics, pp341-354

Dynl RC 1991 'Subsidence resulting from multiple-seam longwall mining under the western United States - A characterization study', Bureau of Mines, United States Department of the Interior: 20

Esterhuizen EC Mark et al 2010 'Numerical model calibration for simulating coal pillars, gob and overburden response' in Proceedings of the 29th International Conference on Ground Control in Mining, Morgantown, WV, pp46-57

Fitzpatrick DJ Reddish DJ et al 1986 'Studies of surface and subsurface ground movements due to longwall mining operations', Proceedings of the 2nd Workshop on Surface Subsidence due to Underground Mining, West Virginia University, Morgantown, WV, pp68-77

Gale WJ 2004 'Multi seam layout guidelines and feasibility of partial chain pillar removal', Australian Coal Association Research Program Report C11032.

Gale WJ 2011 'Investigation into abnormal surface subsidence above longwall panel in the southern coalfield, Australia'in Proceedings of the 30th International Conference on Ground Control in Mining, Morgantown, WV, pp68-77

Holla L 1985 'Surface subsidence prediction in the Southern Coalfield', Mining Subsidence in New South Wales, Department of Mineral Resources, 1: 32

Holla L 1987 'Surface subsidence prediction in the Newcastle Coalfield', Mining Subsidence in New South Wales, Department of Mineral Resources, 2: 30

Holla L 1991 'Surface subsidence prediction in the Western Coalfield', Mining Subsidence in New South Wales, Department of Minerals and Energy, 3: 41

Holla L and Barclay E 2000 'Mine subsidence in the Southern Coalfield, NSW, Australia', NSW Department of Mineral Resources

Kay D and Carter JP 1992 'Effects of subsidence on steep topography and cliff lines' in Proceedings of the 11th International Conference on Ground Control in Mining, University of Wollongong, Wollongong, Australia, pp483-490

Kay DR, McNabb KE et al 1991 'Numerical modelling of mine subsidence at Angus Place Colliery' in Beer, Booker & Carter Computer Methods and Advances in Geomechanics, BCBeer Rotterdam, Balkema

Li G, Steuart P et al 2007 'A case study on multiple-seam subsidence with specific reference to longwall mining under existing longwall goaf' in Proceedings of the 7th Triennial Conference of the Mine Subsidence Technological Society, 26-27 November 2007, University of Wollongong, pp111-125

Lloyd PW, Mohammad N et al 1997 'Surface subsidence prediction techniques for UK coalfields - An innovative numerical modelling approach', Proceedings of the 15th Mining Conference of Turkey, pp111-124

McNally GH, Willey PL et al 1996 'Geological factors influencing longwall-induced subsidence' in Proceedings of the Symposium on Geology in Longwall Mining, University of NSW, Sydney, Australia, pp257-267

Mills K, Waddington AA et al 2009 'Subsidence Engineering' Australian Coal Mining Practice, AusIMM: 874-902

Mine Subsidence Engineering Consultants 2007 'General discussion on systematic and non systematic mine subsidence ground movements', (unpublished)

Mine Subsidence Engineering Consultants 2007 'Introduction to longwall mining and subsidence', (unpublished)

Mine Subsidence Engineering Consultants 2012 'Independent review of subsidence predictions and impact assessments: Upper Liddell Seam - Longwalls 1 to 8 for Ashton Coal Operations Limited', (unpublished)

Mohammad N, Lloyd PW et al 1998 'Application of a UK subsidence numerical modelling methodology to some Australian case studies', Proceedings of the 4th Triennual Conference of the Mine Subsidence Technological Society, 11-13 July 1998, Maitland, pp27-40

Morsy K and Peng SS 2002 'Numerical modelling of the gob loading mechanism in longwall coal mines', Proceedings of the 21st International Conference on Ground Control in Mining, Morgantown, WV, pp58-67

Pappas DM and Mark C 1993 'Behaviour of simulated longwall gob material', Bureau of Mines: 39

Pietruszczak S and Mroz Z 1980 'Numerical analysis of elastic-plastic compression of pillars accounting for material hardening and softening', International Journal of Rock Mechanics and Mining Sciences & Geomechanics Abstracts 17: 199-207

Pietruszczak S and Mroz Z 1981 'Finite element analysis of deformation of strain-softening materials', International Journal for Numerical Methods in Engineering 17: 327-334

Schumann EHR 1987 'Surface subsidence due to multi-seam total extraction at Sigma Colliery' Report to the Strata Control Advisory Committee of the Coal Mining Research Controlling Council: 39

Sheorey PR, Loui JP et al 2000 'Ground subsidence observations and modified influence function method for complete subsidence prediction', International Journal of Rock Mechanics and Mining Sciences 37: pp801-818

Smart BGD and Haley SM 1987 'Further development of the roof strata tilt concept for pack design and the estimation of stress development in a caved waste', Mining Science and Technology 5: 121-130

Su DWH 1991 'Finite element modelling of subsidence induced by underground coal mining: The influence of material nonlinearity and shearing along existing planes of weakness' in Proceedings of the 10th International Conference of Ground Control in Mining, Morgantown, WV, pp287-300

Suchowerska AM 2014 'Geomechanics of single-seam and multi-seam longwall coal mining'. University of Newcastle, University of Newcastle, submitted PhD thesis for examination

te Kook J , Scior C et al 2008 'Subsidence prediction for multiple seam extraction under consideration of time effects by the use of geomechanical numerical models' in Proceedings of the 27th International Conference on Ground Control in Mining, Morgantown, WV, pp143-147

Trueman R 1990 'A finite element analysis for the establishment of stress development in a coal mine caved waste', Mining Science and Technology 10: 247-252

Vakili A, Albrecht J et al 2010 'Mine-scale numerical modelling of longwall operations', 10th Underground Coal Operators' Conference, Wollongong NSW, pp115-124

Wardle LJ and Enever JR 1983 'Application of the displacement discontinuity method to the planning of coal mine layouts', Proceedings of the 5th International Congress on Rock Mechanics, Melbourne, Australia, pp E64-E69

Wilson AH 1980 'Stability of underground workings in the soft rocks of the coal measures', Nottingham, Nottingham University PhD Thesis

Yu H-S 2010 Plasticity and Geotechnics, Springer Science+Business Media